Modulation Schemes in Low-Cost Microwave Field Sensors

PETER A. JEFFORD AND MICHAEL J. HOWES

***Abstract*—The use of modulation schemes in short-range microwave field sensors are discussed and in particular the ideas are applied to low-cost self-detecting doppler sensors based on a two-terminal negative resistance diode oscillator which acts as a load variation detector. FM–CW and pulse modulation techniques are described which can lead to improved performance in these sensors, and experimental results of bias modulation, varactor modulation, and pulsed operation of transferred-electron oscillators are presented. Modulation techniques can be applied in order to eliminate false alarms due to unwanted targets by enabling the doppler sensor to measure or discriminate target range, and the potential merits of different schemes based on frequency modulation with linear and sinusoidal modulation patterns are explored. A novel environmental profiling technique is proposed which exploits the response of frequency-modulated sensors to multiple stationary targets for use in a versatile short-range surveillance system employing digital processing techniques. The mechanism of pulsed operation in self-detecting sensors is described, and the effects of temperature variations in the active device, which result in frequency chirp, are considered. The technique of extracting the doppler signal from the pulsed bias current using a pulse cancellation circuit is demonstrated, and the effects of bias current changes during the pulse (due to temperature variations) on the use of this type of circuit are discussed.**

List of Symbols

δV_B	small signal voltage changes in bias circuit
l_0	distance of target from oscillator
v_r	velocity of moving reflector
K	constant
R_B	bias resistance
l	length
ω, ω_0	angular frequency
c	velocity of light
t	time
ω_0'	rate of change of angular frequency
ω_r, ω_d	angular frequencies (due to range and doppler)
ϕ_0, ϕ_m	phase angles
l_{sc}	short circuit length
f, f_0	frequency
P_0	power
I	current
V_B	bias voltage
V_V	varactor reverse bias voltage
δf	frequency change
δI	current change
d_0	distance from antenna
τ	time interval, pulse length
f_r, f_d	frequencies (due to range and doppler)
f_m	modulation frequency
Δf	frequency excursion
n	number of samples
f_{max}	maximum frequency
$\Delta\omega$	angular frequency excursion
ω_m	angular modulation frequency
$J_0(D), J_1(D)$	
$J_2(D), J_n(D)$	Bessel functions of argument D
x	variable
V_{BO}	pulse peak voltage
$v(t)$	time varying voltage
T_m	pulse period
m	modulation index
τ'	effective pulse length

Manuscript received July 22, 1982; revised April 5, 1983.
P. A. Jefford is with the Royal Signals and Radar Establishment, Malvern, Worcesterchire, England.
M. J. Howes is with the Department of Electrical and Electronic Engineering, Leeds University, Leeds, England.

I. Introduction

MODULATION schemes based on conventional pulse or FM–CW radar techniques have been employed in short-range doppler detection systems [1]–[3], and the use of such modulation patterns can offer significant improvement on the basic CW system. The simplest form of doppler sensor, which can be realized at a lower cost than a separate mixer design, consists of a CW oscillator radiating power through an antenna, with the same diode serving as both the oscillator of the transmitter and as a mixer in the receiver. The transferred-electron device (TED), IMPATT diode, and BARITT diode have the necessary characteristics to carry out this function [4]–[9]. A moving reflector in the field of the antenna is seen as a variation of the microwave load impedance by the oscillating diode and this gives rise to power and frequency changes in the oscillator [10]. In a transferred-electron oscillator (TEO) these changes modulate the current through the diode at the doppler frequency, and by inserting a series resistor in the bias line this doppler signal is detected as a voltage variation at the diode terminals.

Microwave field sensors have found wide commercial application as doppler intruder alarms where cost and size are important considerations in the choice of system design. A severe problem of doppler sensors in this application is that of false alarms due to unwanted targets, such as near flying insects, or to movement caused by air turbulence or vibration. The basic CW doppler detector cannot distinguish between a man target at long-range and a much smaller object, such as an insect, at close-range, and intruder alarm systems may incorporate energy-integrating circuits or time-delay triggering circuits to minimize the occurrence of false alarms [11], [12]. The use of digital analysis techniques, to recognize certain target characteristics from their doppler signals, has also been reported [13]. However, the use of modulation techniques in the doppler sensor provides a means of eliminating false alarms by range discrimination and by indication of the direction sense.

Previous research has been concerned with the use of modulation schemes in doppler radar systems, which employ separate transmitter and receiver circuits, for automobile applications [1], [2], and in man-portable surveillance radar [3]. Both triangular FM–CW and FM-pulse modulation have been used in experimental automobile radar [1], [2] in order to measure target range and velocity. The FM-pulse technique uses alternate transmission at two slightly different microwave frequencies and parallel processing in two separate channels to provide range and direction sense information. Pulsed operation (or more correctly, intermittent CW operation) not only leads to a saving in dc power, but also means that targets whose radar delay time is greater than the pulse length are not detected, and this range cutoff effect can be used to eliminate false alarms due to distant objects. The dual frequency technique has also been demonstrated in a microstrip CW self-detecting sensor based on a BARITT oscillator [14] by square-wave switching the diode current between two different bias levels. Sinusoidal FM techniques have been used in sophisticated man-portable surveillance radars [3] in order to achieve signal detection which is independent of range out to about two-thirds of maximum range, due to the range discrimination characteristics of sinusoidal FM–CW radar [15].

This paper is concerned with the evaluation of modulation schemes in low-cost microwave field sensors, and in particular the ideas are applied to self-detecting sensors based on a two-terminal negative resistance diode oscillator such as the TEO. The modulation schemes described fall into two basic categories, namely, frequency modulation achieved by bias tuning or varactor tuning, and pulsed or intermittent CW operation where the bias supply to the active device is switched on and off. Experimental results have been obtained by frequency modulation and pulsed operation of waveguide TEO's, and the potential advantages to be gained by the various modulation schemes are explored.

II. Frequency Modulation With Linear Waveforms

Frequency modulation of a CW radar, resulting in a broadening of the transmitted spectrum, enables the radar to measure range as well as velocity, and the techniques of FM–CW radar are well known [15]. In principle the applied frequency modulating waveform may take any form, but the techniques most widely used may be divided into those employing linear modulation patterns, such as triangular FM, and those with nonlinear patterns, such as sinusoidal FM.

A. Frequency Modulation Applied to Self-Detecting Sensors

Consider the case of a self-detecting field sensor where there is no separate mixer and the oscillator behaves as a load variation detector. From the analysis of doppler signal detection by a negative resistance diode oscillator, such as the TEO [5], [7], [10], we have an expression for the detected signal voltage δV_B in the bias circuit due to a target at a distance l_0 from the oscillator moving with uniform velocity v_r away from the antenna

$$\delta V_B = KR_B \cos\frac{(2l\omega)}{c} \tag{1}$$

where K is a constant for a particular oscillator and target reflection, R_B is the value of the series bias resistance, ω is the angular frequency of oscillation, and l is a function of time $(= l_0 + v_r t)$. Let us now assume that pure linear frequency modulation is applied to the oscillator such that the free-running frequency can be expressed as

$$\omega = \omega_0 + \frac{d\omega_0}{dt}\cdot t = \omega_0 + \omega_0' t \tag{2}$$

where ω_0' is the rate of change of frequency due to the modulation. If we neglect the effects of the small frequency variations in the oscillator at the doppler frequency due to the moving target and substitute for ω in (1), we have

$$\begin{aligned}\delta V_B &= KR_B \cos\left[\frac{2l}{c}\cdot(\omega_0 + \omega_0' t)\right]\\ &= KR_B \cos\left[(\omega_r + \omega_d)t + \phi_0\right]\end{aligned} \tag{3}$$

where

$$\omega_r = 2l_0\omega_0'/c,\ \omega_d = 2v_r\omega/c$$

and

$$\phi_0 = 2l_0\omega_0/c.$$

Equation (3) contains both range and velocity information for the moving target. The frequency component ω_r is due to the target range (l_0), ω_d is the doppler frequency component due to the target velocity, and ϕ_0 is a phase angle which is constant in time. The frequency of the detected signal is $(\omega_r + \omega_d)$, which corresponds exactly to the beat frequency obtained in the case of a separate-mixer system. It can be shown that the techniques of triangular FM, and of FM waveforms of other shapes, are directly applicable to self-detecting field sensors. However, pure linear FM is difficult to realize in these oscillators, and although linearity can be achieved by waveform shaping, the notable effects of amplitude modulation must be considered.

B. Modulation in Transferred Electron Oscillators

In order to investigate the use of modulation schemes in self-detecting field sensors, experimental results have been obtained with J-band waveguide TEO's which behave as load variation detectors when the output power is transmitted from a horn antenna and a series resistor is inserted in the bias line. Reflecting targets within the antenna field of view modulate the bias current through the device and the doppler signal is detected as a voltage waveform at the device terminals. The steady-state oscillation frequency of a TED operated in a microwave circuit is determined by the condition that the susceptance of the device be matched by the susceptance of the circuit, which is usually a function of frequency only. Thus, the oscillation frequency can be controlled by changing the circuit susceptance, as in mechanical tuning, varactor tuning, or YIG tuning, or by changing the device susceptance. The value of the device susceptance is determined by many independent factors including the device parameters (such as doping density, active length, and device area), temperature, and applied bias voltage.

Experimentally, it is found that the bias-tuning characteristics of TEO's are circuit-dependent, and that the oscillation frequency and power may exhibit positive and/or negative tuning. The associated frequency modulation sensitivity is defined as the rate of change of oscillation frequency with bias voltage, and values up to 120 MHz/V have been achieved experimentally for X-band devices [16]–[18], although a more typical value might be of the order of 10 MHz/V. The modulation bandwidth is dependent on the circuit Q-factor, and a typical value might be 70 MHz for an X-band device in a resonant circuit with $Q = 200$. Within this bandwidth any modulation can be considered as bias tuning, but for higher modulation rates the FM sensitivity can be expected to decrease.

Bias voltage tuning is attractive in terms of simplicity and cost because it requires no additional microwave circuitry but it tends to be unpredictable and the tuning characteristics can vary considerably from one device to the next. Advantages of using varactor diodes as tuning elements are their low power requirements, small size, and their ability to respond to fast modulation rates. Unfortunately, they have nonlinear capacitance–voltage characteristics and low Q at microwave frequencies, but more predictable and wider tuning ranges can be achieved compared with bias voltage tuning methods.

Measured tuning characteristics are shown in Figs. 1 and 2 for a bias-voltage-tuned TEO and a varactor-tuned TEO, respectively. The oscillators were based on a GaAs TED mounted by means of a cylindrical post in a J-band waveguide cavity. The post diameters are 3.6 mm in the bias-tuned oscillator and 3.0 mm in the varactor-tuned cavity. The TED is mounted in an S4 package at the center of the broad dimension of the waveguide under the post. The dc bias is applied to the TED via an RF choke, and the oscillation frequency can be controlled by means of an adjustable short circuit which determines the length l_{sc} of the waveguide cavity. The first oscillator is tuned by varying the dc bias voltage of the TED, and the other oscillator includes a varactor diode mounted under a second 3-mm diameter post at a distance of 14.6 mm along the guide center line away from the TED post and towards the output port. The varactor diode is contained in an S4 package and a second RF choke is used to apply the tuning

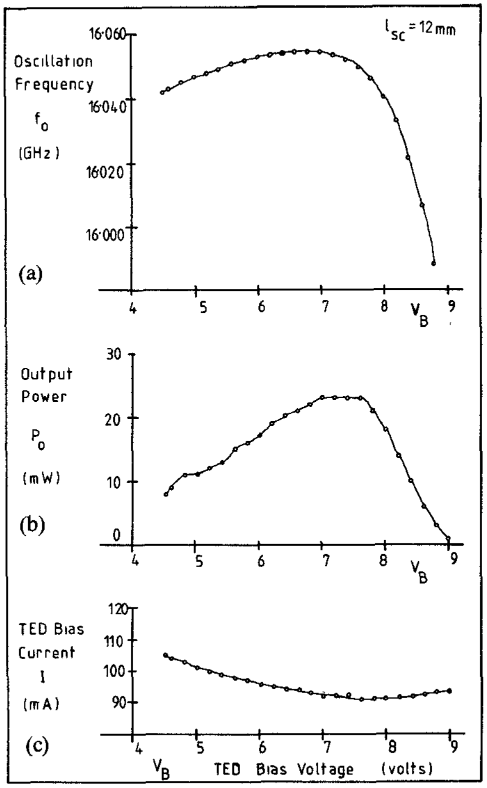

Fig. 1. Measured dc bias voltage tuning characteristics for the transferred electron oscillator. (a) Oscillation frequency f_0 (GHz). (b) Microwave output power P_0 (mW). (c) TED bias current I (mA).

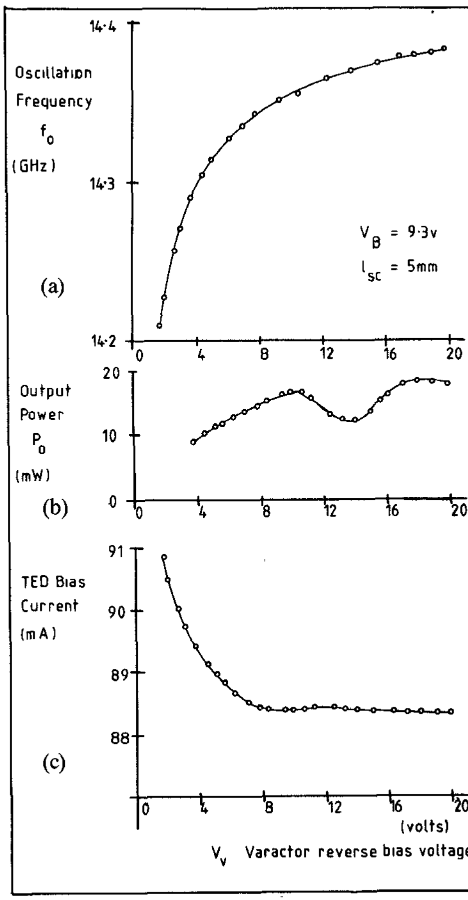

Fig. 2. Measured tuning characteristics for the varactor tuned TEO. (a) Oscillation frequency f_0. (b) Output power P_0. (c) TED bias current.

voltage. The frequency of oscillation is determined approximately by the separation between the two posts, which corresponds to a half-guide-wavelength at 14 GHz, and the movable short circuit facilitates some degree of mechanical tuning. The TED is a J-band n^+-n-n^+ structure with active length 5.9 μm, 70-μm diameter, and 2.5×10^{-21}-m^{-3} doping density, which is bonded, anode down, into the package. The varactor is a Schottky-barrier diode formed on a GaAs substrate with 3-μm epilayer thickness, 10^{22}-m^{-3} doping density, and a Ti–Au contact bonded into the package.

The bias voltage tuning characteristics in Fig. 1 show (a) oscillation frequency f_0, (b) microwave output power P_0, and (c) the TED bias current I plotted against the TED bias voltage V_B. As V_B is increased, the frequency and output power increase to a maximum and then decrease again. In the region where $4.5 < V_B < 7.0$ V, smooth positive tuning is achieved at a rate of approximately 5 MHz/V with output power increasing from 8 mW to 23 mW. Faster tuning with negative $\delta f/\delta V_B$ occurs for $V_B > 7.0$ V, but in this region the power drops off more sharply. If the modulated TEO is to be operated as a self-detecting doppler sensor, then the effect of tuning on the sampled bias current is very significant. In Fig. 2(c) the rate of change of TED current with applied bias voltage $(\delta I/\delta V_B)$ is approximately -5 mA/V in the region of positive tuning, and $+3$ mA/V in the region of negative tuning. The varactor tuning curves in Fig. 2(a) and (b) shows that wider tuning ranges can be achieved in this oscillator with less variation in output power ($\sim$160 MHz tuning with $9 < P_0 < 18$ mW), but modulations of several mA still occur in the TED bias current as shown in Fig. 2(c). This means that when a modulating voltage is applied to the bias terminals of the TED or to the varactor terminals, the corresponding TED bias-current variation is of the order of a few microamps, compared with the small bias-current variations occurring at the doppler frequency due to a moving target. The doppler signal current could be of the order of microamps or less. The presence of large cross-modulation currents in the bias circuit at the modulation frequency and its harmonics make it very difficult to extract and measure the instantaneous beat frequencies in order to determine target range and velocity using linear FM waveforms in a self-detecting sensor.

Equations (1) and (3) expressed the doppler signal voltage δV_B in a self-detecting sensor based on a TEO in terms of a constant K, the bias resistance, and a cosine function. However, the value of K is dependent upon the sensitivity of the oscillator to load changes, and on the effective reflection coefficient of the target [10]. If the oscillator frequency is modulated by applying a voltage waveform to the TED bias or to a varactor in the circuit, and this applied signal also gives rise to amplitude modulations, then the sensitivity of the oscillator to load variations will change according to the applied voltage. The value of K is no longer constant and the doppler signal is amplitude modulated by the applied waveform. Fig. 3 shows the effect of (a) TED bias tuning and (b) varactor tuning on the amplitude of the measured doppler signal due to a moving target simulated by a rotating paddle wheel, consisting of a cylinder with radially mounted aluminium vanes at a distance of 60 cm from the antenna. Fig. 3(a) shows the voltage of the doppler signal across the bias resistor R_B ($=10\ \Omega$) versus the TED dc bias voltage V_B, and Fig. 3(b) shows the doppler signal versus varactor dc bias voltage for the varactor tuned TEO. These curves show that significant AM sidebands of the doppler signal would result from bias or varactor modulation of the oscillator. These sidebands would occur around the modulation frequency and its harmonics in addition to those signals due to direct modulation of the TED bias current. The resulting spectrum would be complicated and could yield no more information about the target other than that due to the beat frequency $(\omega_r + \omega_d)$ which is a low amplitude component of the spectrum. It is concluded that although the doppler and range measuring procedure would work in principle in self-detecting sensors, the problems of wave-shaping to produce linear FM patterns and the difficulty of filtering to extract the beat frequency components make the technique impractical for use in low-cost sensors.

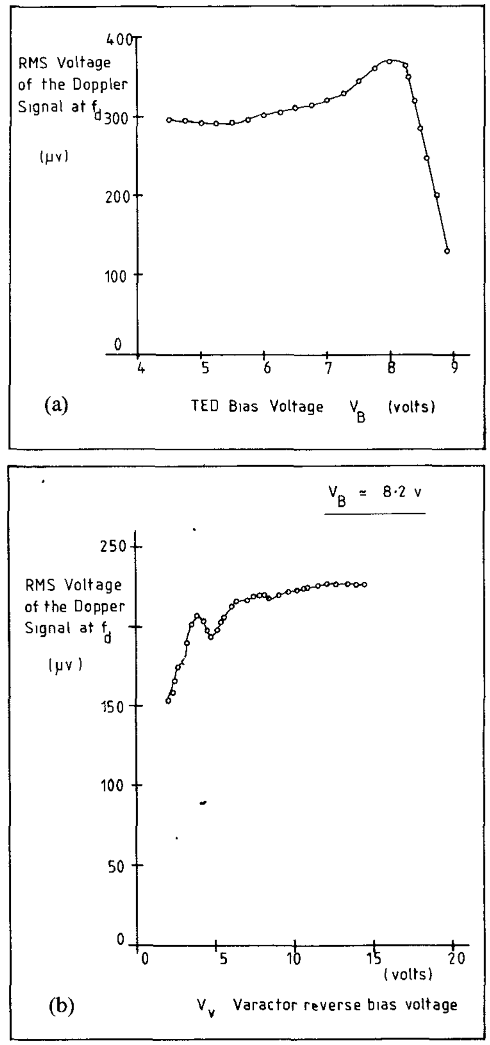

Fig. 3. Graphs showing the effects of (a) TED bias tuning and (b) varactor tuning on the measured doppler signal amplitude.

This is particularly true in a situation where there would be a large number of reflecting objects within the antenna field of view, since stationary reflectors also give rise to beat frequency components, and separation of the individual targets would be difficult.

C. Environment Profiling — A Novel Low-Cost Surveillance Technique

In this section it is proposed to show how the response of a modulated sensor to stationary targets might be exploited in order to detect movement in a novel short-range surveillance system which would have several advantages compared with ordinary motion detectors.

Consider a frequency-modulated microwave field sensor which is to be used as the basis of an intruder detector in a cluttered environment. If the oscillator frequency is linearly modulated, for example, in a sawtooth pattern, then a stationary object at a range d_0 from the antenna results in a beat frequency which varies with time in the manner shown in Fig. 4. During each upsweep of the oscillation frequency over the time interval τ, the beat frequency has a constant value given by $f_r = (4d_0 f_m \Delta f)/c$ where f_m is the modulation rate and Δf is the frequency excursion. If there are many stationary objects within the antenna field of view, then the baseband signal during some gate time interval τ contains many components whose amplitudes and frequencies correspond to the size and range of each target. Thus, a cluttered environment results in a spread of beat frequencies, and the spectrum of the baseband signal during the sample time can be imagined to represent that environment. This spectrum or profile does not change unless the objects within the environment change position or new reflectors are introduced. Comparing the spectra sampled at successive time intervals will allow any change in the environment surveyed by the sensor to be detected. It is proposed that the signal should be processed using an A to D converter and an FFT processor. The gate time τ should be less than the modulation period $1/f_m$ minus the range delay time due to the most distant targets. If the A to D converter samples the gated waveform at intervals τ/n, where n is the total number of samples, then the frequency spectrum can be represented by $n/2$ discrete components. Fig. 4(b) shows a discrete frequency spectrum which might represent the profile of a particular target area. From the sampling theorem the maximum frequency in the discrete spectrum f_{max} is equal to half the sampling frequency, i.e., $f_{max} = n/2\tau$, and the separation between individual spectral lines is $1/\tau$. The value of f_{max} determines the maximum range at which reflecting objects can be monitored, and the system therefore has a cutoff range whose value is determined by the digital sampling rate, Δf, and f_m. For example, if the sensor is modulated over a frequency range $\Delta f = 750$ MHz at a rate $f_m = 100$ Hz, the sampling rate is 125 KHz ($\equiv$ 8-μs sampling time), and the total number of samples is 1024, then the gate length τ is 8.19 ms. The frequency spectrum can be represented by 512 discrete components separated by 122 Hz and f_{max} is 62.5 KHz, so that only targets up to a range of 62.5 m would be monitored and the range resolution would be approximately 12 cm. Since the beat frequency for a particular reflector is related only to range delay when $f_d \ll f_r$, the system can determine the corresponding distance to a disturbance in the environment, within the limits of range resolution, and can therefore be range selective in order to eliminate false alarms due to unwanted targets. Good tuning linearity in the sensor is not essential for effective operation of the system, although the accuracy of the range discrimination is determined by that linearity. The effects of spurious modulation components and harmonics in the beat frequency signal are not likely to be critical and these can be removed in the processor. Similarly the repeatability of performance from one sensor to another is not critical and therefore the microwave field sensors themselves may be relatively low-cost items.

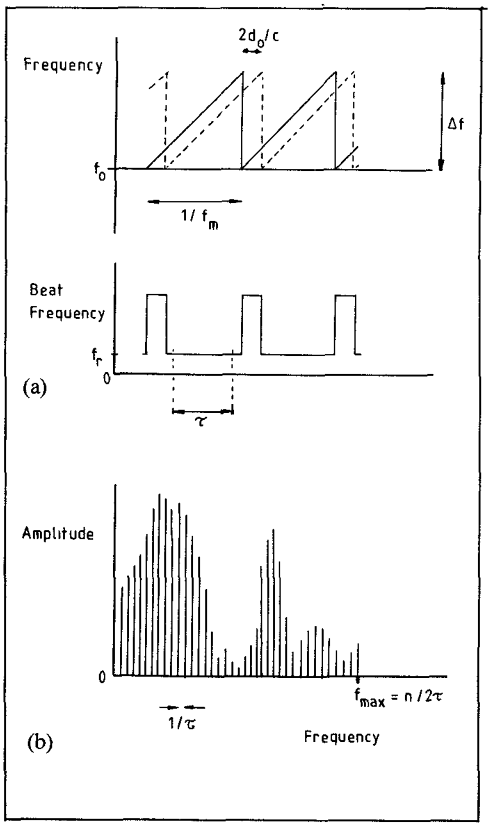

Fig. 4. (a) Frequency versus time relationships for a sensor employing a sawtooth frequency modulation pattern and (b) an example of a discrete frequency spectrum which might represent the profile of a particular target area.

The use of digital processing with this type of surveillance sensor makes the system extremely versatile both in possible applications and in operation. The processing might be carried out using custom-built hardware, although a standard commercial microcomputer with appropriate software might be a cheaper alternative. A single processor with suitable memory may be used to monitor any number of sensors which are interrogated sequentially for comparison with previously stored profiles, allowing continuous surveillance over a large area. The computing time associated with each interrogation may run into seconds, although the use of custom-built hardware, particularly using 16-bit microprocessors, could increase the speed. The advancing technology and falling costs of digital processing hardware make this type of surveillance system with its ability to discriminate target range an attractive proposition.

III. Sinusoidal Frequency Modulation

If the CW carrier of a doppler radar is modulated by a sine wave, the beat frequency obtained due to a single moving target may be expanded in a trigonometric series whose terms are the harmonics of the modulating frequency f_m [15]. If the transmitted signal is of the form

$$\sin\left[\omega_0 t + (\Delta\omega / 2\omega_m)\cdot \sin \omega_m t\right]$$

where ω_0 is the carrier frequency, ω_m is the modulation frequency, and $\Delta\omega$ is the angular frequency excursion, then the difference frequency signal may be written

$$\begin{aligned} v_d = {} & J_0(D)\cos(\omega_d t + \phi_0) \\ & -2J_1(D)\sin(\omega_d t + \phi_0)\cdot\cos(\omega_m t - \phi_m) \\ & -2J_2(D)\cos(\omega_d t + \phi_0)\cdot\cos 2(\omega_m t - \phi_m) \\ & +2J_3(D)\sin(\omega_d t + \phi_0)\cdot\cos 3(\omega_m t - \phi_m) \\ & +2J_4(D)\cos(\omega_d t + \phi_0)\cdot\cos 4(\omega_m t - \phi_m) \\ & + \cdots \end{aligned} \tag{4}$$

where J_0, J_1, J_2, etc., are Bessel functions of the first kind and order 0, 1, 2, etc., respectively, $D = (\Delta\omega/\omega_m)\sin(\omega_m d_0/c) \simeq (\Delta\omega_m d_0/c)$ for small $\omega_m d_0/c$, d_0 = distance to the target at time $t = 0$ (the distance that would be measured if the target were stationary), $\omega_d = 2v_r\omega_0/c$ = doppler frequency shift ($\ll \omega_m$), v_r = relative velocity of the target with respect to the radar antenna, ϕ_0 = phase shift approximately equal to the angular distance $2\,\omega_0 d_0/c$, and ϕ_m = phase shift approximately equal to $\omega_m d_0/c$. The beat frequency signal of (4) consists of a doppler frequency component of amplitude $J_0(D)$ and a series of cosine waves of frequency f_m, $2f_m$, $3f_m$, etc. Each of these harmonics of f_m is modulated by a doppler frequency component with amplitude proportional to $J_n(D)$. The product of the doppler frequency factor and the nth harmonic factor is equivalent to a suppressed carrier double sideband modulation. The spectrum of the beat frequency signal is shown in Fig. 5(a) and, in principle, any of the J_n components of the difference frequency signal can be extracted to yield doppler information. Fig. 5(b) shows a plot of several of the Bessel functions whose values form the coefficients of the individual components. The argument D of the Bessel function is dependent on target range and can be written as

$$D = (\Delta f / f_m)\sin 2\pi/(d_0/\lambda_m) \tag{5}$$

where $\lambda_m = c/f_m$. It can be seen from Fig. 5(b) and (5) that each harmonic component has a range dependence, in addition to the normal $1/R^4$ range power law, such that a suitable choice of Δf and f_m for a particular harmonic component can result in emphasis or de-emphasis of the output for certain target ranges. For example, when only a single target is involved, the frequency excursion Δf can be adjusted to obtain that value of D which places the maximum of the appropriate Bessel function at the target range.

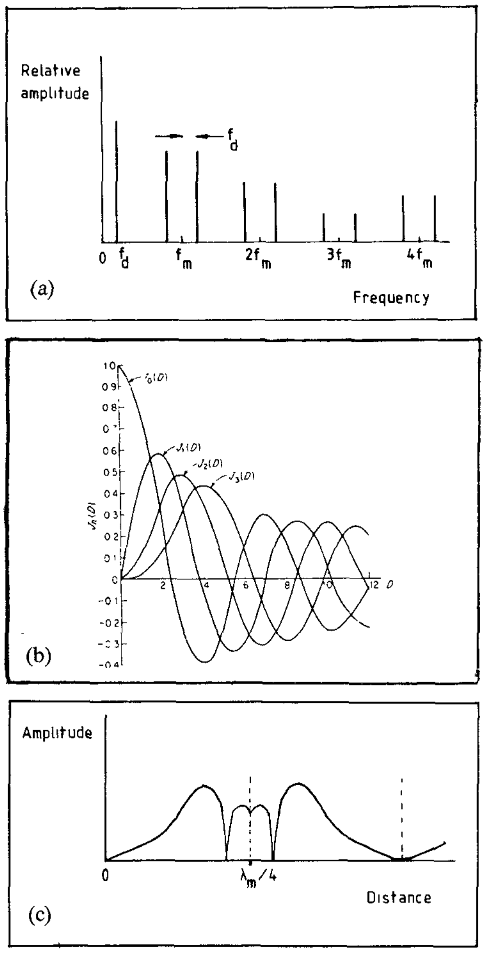

Fig. 5. (a) Spectrum of the beat frequency signal obtained from a sinusoidally modulated FM–CW radar, (b) a plot of Bessel functions of order 0, 1, 2, and 3, and (c) a plot of $J_3(D)$ as a function of distance.

A plot of $J_3(D)$ as a function of distance is shown in Fig. 5(c). The curve is mirrored because of the periodicity of D. (The mirror distance is $\lambda_m/4$.) The nulls in the curve suggest that the response due to targets at certain ranges can be suppressed by the proper choice of modulation parameters, and false alarms due to unwanted targets at these ranges can therefore be eliminated. It should be noted that it is a property of Bessel functions that $J_n(x)$, for $n \neq 0$, varies as x^n for small x, and this property can be exploited to counteract the normal R^4 range law.

A. Experimental Results in Self-Detecting Sensors

The effects of sinusoidal frequency modulation were investigated in the bias voltage tuned and varactor tuned TEO's using the rotating paddle wheel as a moving target. In both cases the amplitudes of the baseband and harmonic sideband doppler signal voltages across the bias resistor R_B ($=10\ \Omega$) were measured using an FFT spectrum analyzer. The moving target was positioned at a distance $d_0 = 1.5$ m from the antenna and rotated at speed which resulted in a major peak of doppler at $f_d = 300$ Hz. A sinusoidal modulating voltage was applied to the TED via a bias transformer, and the RF frequency deviation Δf was increased

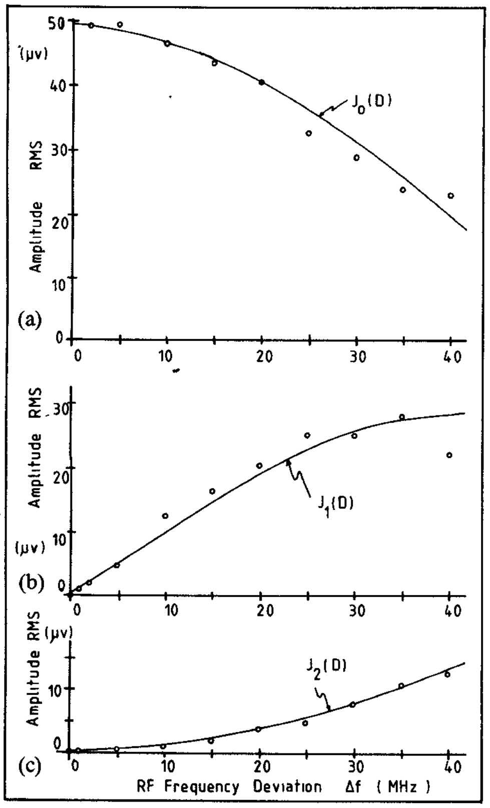

Fig. 6. Measured amplitude versus RF frequency deviation characteristics for the doppler components at frequencies (a) baseband f_d, (b) $f_m + f_d$, and (c) $2f_m + f_d$ in the bias voltage tuned TEO with a moving target, and the corresponding theoretical Bessel function curves.

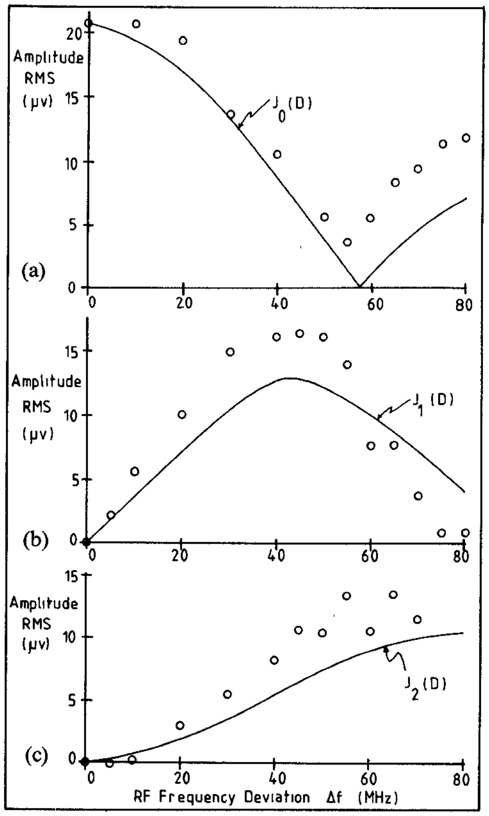

Fig. 7. Measured doppler signal component amplitudes versus RF frequency deviation in the varactor tuned TEO at frequencies (a) f_d, (b) $f_m + f_d$, and (c) $2f_m + f_d$, and the corresponding theoretical Bessel function curves.

from zero to 40 MHz by increasing the amplitude of the ac bias modulation from 0 to 3.2 V peak-to-peak. The TED dc bias was 5.7 V and the modulation frequency $f_m = 10$ KHz. The graphs in Fig. 6 show the voltage amplitude of (a) the baseband doppler signal at f_d, and the harmonic sideband at frequencies (b) $f_m + f_d$ and (c) $2f_m + f_d$ plotted against frequency deviation Δf. The three graphs correspond to the Bessel functions $J_0(D)$, $J_1(D)$, and $J_2(D)$, respectively, since the parameter D is given by

$$D = (\Delta f / f_m)\sin(2\pi f_m d_0 / c)$$
$$\simeq 2\pi \Delta f d_0 / c \qquad \text{for small } f_m \ (f_m \ll c/d_0). \qquad (6)$$

There is good agreement between the experimental points and the theoretical Bessel function curves (J_0, J_1, and J_2,) which are normalized to $J_0(0)$ as shown. Fig. 7 shows the corresponding results for the varactor tuned TEO where the varactor bias voltage was sinusoidally modulated from 0 to 8 V peak-to-peak producing up to 80-MHz frequency excursion. In this case, the agreement between the theoretical curves and the experimental points is not as close as in the bias modulated TEO, and this is mainly due to the nonlinearity in the varactor tuned characteristic compared with the bias tuned oscillator. Additional sources of discrepancy between the experimental results and theory are due to the effects of amplitude modulation in the oscillator and additional frequency modulation of the oscillator due to the moving target. The effects of cross-modulation described in Section II-B where the applied modulation results in corresponding modulation of the TED bias current does not significantly affect the technique of range discrimination using sinusoidal FM-CW operation. The result of the cross-modulation is that, in addition to the spectral components shown in Fig. 5(a), there are fixed amplitude components at frequency f_m and at the harmonics of f_m. Stationary targets also result in 'zero-doppler' components at frequencies f_m, $2f_m$, $3f_m$, etc., with amplitudes according to the value of the corresponding Bessel function and their distance from the oscillator. It will be seen that these zero-doppler components can be rejected in the processing circuits.

The results shown in Fig. 8 were obtained by keeping the frequency deviation constant ($\Delta f = 70$ MHz) in the varactor tuned oscillator and increasing the target range d_0 from 0.2 m to 1.6 m. The voltage amplitude is multiplied by d_0^2 and plotted against d_0 in order to eliminate the effect of the normal range law where the doppler signal amplitude is proportional to $1/d_0^2$. The three graphs (a), (b), and (c) represent the amplitude versus range dependencies of the baseband doppler signal at f_d, and the components at frequencies $f_m + f_d$ and $2f_m + f_d$ corresponding to the J_0, J_1, and J_2 Bessel functions, respectively. This technique of range discrimination using sinusoidal FM could be implemented in a motion detector system based on a self-detecting field sensor, by using the J_n component (where $n = 1, 2, 3$, etc., as required) extracted by a narrow-band filter centered on the nth harmonic of f_m, and employing a mixer to down-convert this signal to baseband as shown in

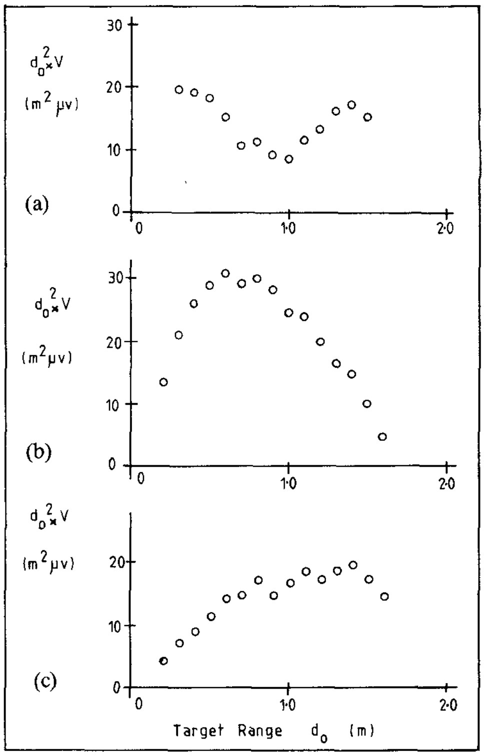

Fig. 8. Graphs showing the measured amplitude versus target range characteristics for the doppler components at frequencies (a) baseband f_d, (b) $f_m + f_d$, and (c) $2f_m + f_d$ in the varactor tuned TEO when $\Delta f = 70$ MHz.

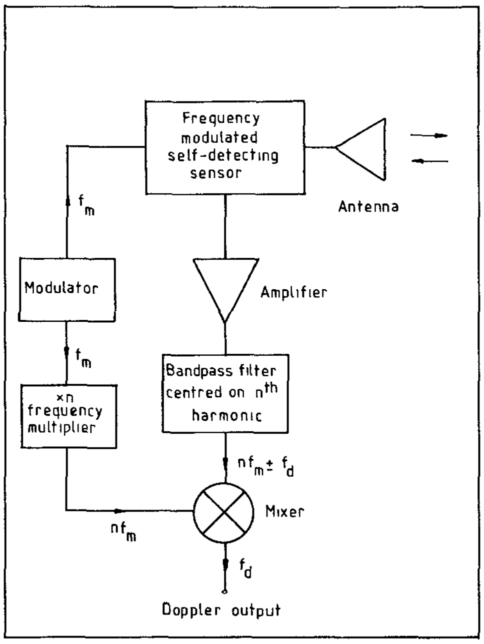

Fig. 9. Block diagram showing the implementation of sinusoidal FM range discrimination in a self-detecting doppler sensor.

Fig. 9. The doppler output can be processed in the normal ways and possible schemes are:

a) to extract the J_0 component by means of a low-pass filter in order to exploit the rapid fall-off in response with increasing distance, thereby detecting only close targets;
b) to extract a higher order J_n component and exploit the response characteristic to define a preferred range band for detection; or
c) to use the response nulls to eliminate the detection of targets at certain ranges.

The use of such schemes can reduce the false alarm rate in a motion detector by enabling the system to discriminate range. Inspection of (6) shows that values of Δf less than 70 MHz and low modulation rates would be sufficient for most applications, and therefore either simple bias-voltage tuning or varactor tuning could be employed to modulate the oscillator.

The technique described above features another significant advantage when the higher order Bessel function components are extracted because of the $1/f$ noise power density spectrum which is characteristic of these semiconductor devices. At baseband doppler frequencies, the $1/f$ noise contribution in the bias circuit of the active device is large, but at the higher frequency harmonics of $n \cdot f_m$ the noise power is reduced by a factor of f_d/nf_m. By proper choice of modulation parameters, the noise reduction can lead to an improvement in sensitivity for certain target ranges, although the total energy contained in the beat signal is distributed among all the harmonics and extracting just one component wastes signal energy in the other harmonics.

IV. Pulse Modulation in Self-Detecting Field Sensors

Techniques of pulse doppler radar which detect moving targets in stationary clutter are well understood, but pulsed operation of self-detecting sensors is a rather different situation. The basic circuit configuration of a pulsed self-detecting sensor based on a TED in a waveguide cavity is shown in Fig. 10(a). The idealized voltage waveforms appearing across the device terminals are shown in Fig. 10(b) for different target situations. The effects of rise-time, delay-time, and fall-time in the oscillator are neglected, and it is assumed for the moment that the bias current I and oscillation frequency ω_0 remain constant during each pulse of the applied waveform if there are no reflecting objects within the antenna field of view. In Fig. 10(b), (ii) shows the voltage waveform across the device terminals when no targets are present within the antenna field, and it consists of rectangular pulses of height V_{BO} corresponding to the applied rectangular pulses in (i). A stationary reflecting target at a distance d_0 from the antenna presents a different load admittance to the oscillator, and the bias current takes on a new value during the pulse. The bias voltage V_B changes by an amount δV_B because of the series bias resistor R_B, but the radar delay time associated with target range means that the voltage remains constant at V_{BO} for a period of time ($= 2d_0/c$) at the beginning of the pulse (iii). The voltage change δV_B can be positive or negative depending on the distance to the reflector in RF wavelengths.

If the target is moving with a velocity v_r relative to the

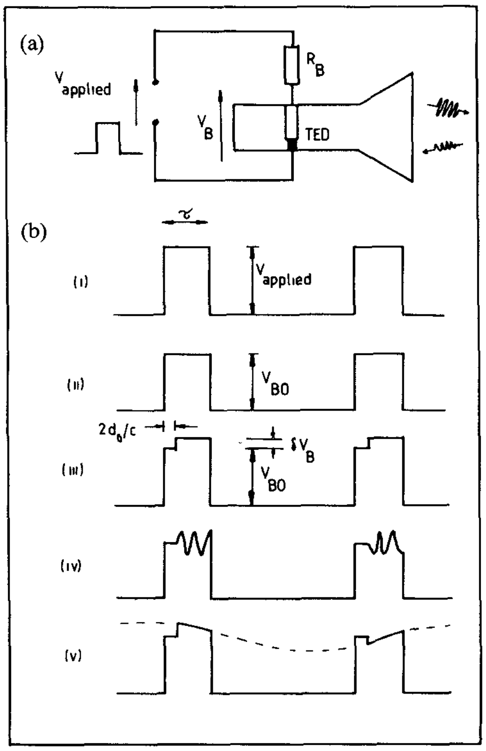

Fig. 10. (a) Basic circuit configuration of a pulsed self-detecting field sensor and (b) idealized voltage waveforms for the circuit in (a): (i) applied voltage, (ii) detected pulse train when there are no targets present, (iii) detected pulse train for a stationary target at range d_0, (iv) target moving with $f_d > 1/\tau$ and (v) $f_d < 1/\tau$.

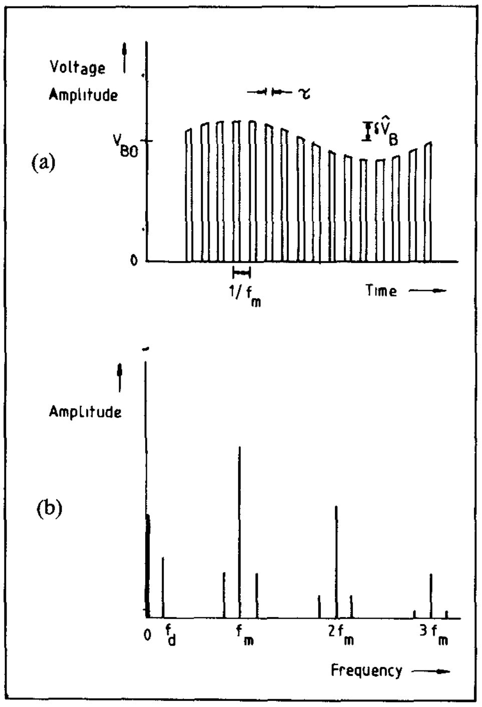

Fig. 11. (a) The PAM waveform where the voltage pulses across the TED are amplitude modulated at the doppler frequency f_d due to a moving target and (b) the corresponding frequency spectrum.

antenna then the latter portion of the voltage pulses are amplitude modulated at the doppler frequency as shown in Fig. 10(b) (iv) for $f_d > 1/\tau$ and (v) for $f_d < 1/\tau$. Targets at distances greater than $\tau c/2$ are not detected at all and, for example, the cutoff range for a 500-ns pulse is 75 m.

If the radar delay time for a particular target is negligible compared to the pulse length, then the voltage pulses across the TED are amplitude modulated at the doppler frequency as shown in Fig. 11(a). The voltage of a pulse amplitude modulated (PAM) waveform can be expressed as

$$v(t) = \frac{\tau}{T_m} + \frac{\tau}{T_m}\sin\omega_d t + \frac{2\tau}{T_m}\sum_{n=1}^{\infty}\frac{\sin x}{x}\cdot\cos n\omega_m t + \frac{m\tau}{T_m}\sum_{n=1}^{\infty}\frac{\sin x}{x}\left[\sin(\omega_m+\omega_d)t + \sin(\omega_m-\omega_d)t\right] \quad (7)$$

where T_m is the pulse period ($=1/f_m$), m is the modulation index ($=\delta\hat{V}_B/V_{BO}$), and $x = n\omega_m\tau/2$. The frequency spectrum of this waveform is shown in Fig. 11(b). The unmodulated train (when $m=0$) consists of a set of discrete frequency components at f_m, $2f_m$, $3f_m$, etc., and, due to amplitude modulation at the doppler frequency, each of these harmonic components will have an upper and lower doppler sideband component. The amplitudes of the harmonic components and their sidebands follow the normal $\sin x/x$ function, but when the radar delay time for the target is significant compared with the pulse width, the amplitudes of the baseband doppler component and the doppler sidebands are reduced accordingly. As the distance to the target increases up to the cutoff range, the amplitudes of these doppler components decrease in addition to the normal range law.

In principle, the baseband doppler frequency component at f_d can be extracted using a low-pass filter and its amplitude is proportional to $m\tau' f_m$ where the effective pulse length τ' is equal to the pulse width τ minus the radar delay time for the target. However, the value of modulation index m for normal oscillator and targets might be of the order of -100 dB or less, and since the amplitude of the baseband doppler component is related to the amplitude of the harmonic components of f_m by $m\tau'/\tau$, it is not practical to filter out the baseband doppler signal directly. The effective modulation index can be increased by subtracting unmodulated pulses, whose voltage amplitudes are approximately equal to V_{BO}, in a differential amplifier cancellation circuit. This technique results in an output signal whose spectrum is similar to that shown in Fig. 11(b) but where the amplitudes of the modulation harmonics components at frequencies f_m, $2f_m$, $3f_m$, etc., are reduced according to the cancellation factor. The amplitudes of the doppler components are unaffected and the baseband doppler signal can be more readily isolated using a low-pass filter.

A. The Effects of Chirp in Pulsed Field Sensors

In the discussion so far the effects of temperature variations in the active device during the application of the bias voltage pulse have been neglected. The rise in active layer temperature over the pulse width results in changes of oscillation frequency (chirp), output power, efficiency, and bias current during the RF pulse. The effects of the frequency change during the pulse can be understood by reference to the discussion on frequency modulation in Section III. Frequency modulation of the transmitted waveform results in doppler signal components appearing at frequencies $nf_m \pm f_d$ in addition to those shown in the PAM spectrum of Fig. 11(b). In general, for normal operation this effect can be neglected when the baseband doppler signal is extracted, but in the case of FM-pulse operation even small frequency variations during the pulse can be unacceptable [2]. Elimination of chirp is important in this case because of the small frequency difference between alternate pulses which enables phase comparison between the two doppler signals in order to measure target range.

A further problem associated with chirp in pulsed self-detecting field sensors is due to the change in bias current caused by temperature variations during the pulse. The bias pulse cancellation technique described earlier is based on the use of a differential amplifier circuit which allows the extraction, by filtering, of the doppler signal from the bias voltage waveform. The effectiveness of this technique relies on obtaining voltage pulses of similar shape to the original TED bias pulses and subtracting these from the doppler modulated pulse train in the comparator circuit. Variations in the TED bias current during the pulse lead to nonuniform bias voltage pulses because of the series resistor. If the reference voltage pulses are derived from the applied modulating waveform through a dummy (resistive) load as shown in Fig. 12, then these will be different in shape from the TED bias pulses. The spectrum of the differential amplifier output signal will therefore contain residual harmonics of the pulse-modulation frequency. This effect is illustrated in Fig. 13 where measured spectra of the bias voltage waveforms are shown for the J-band waveguide TEO described in Section II-B when 10-V 50-μs pulses are applied at a repetition rate of 2.5 KHz. The TED was a standard CW device and the measured frequency chirp was -20 MHz for a 50-μs pulse. Fig. 13 shows the spectrum of the amplifier output waveform (a) without pulse cancellation and (b) with pulse subtraction. Approximately 40-dB cancellation is achieved at 2.5 KHz ($= f_m$), and only 1.2 dB at 20 KHz ($= 8f_m$), and although this cancellation is sufficient to enable measurement of doppler signals for very close moving targets, it is not adequate for a sensitive motion detector. The amplitudes of the harmonic residuals were up to 30-dB greater than the baseband doppler component measured for the revolving target at a distance of 20 cm from the antenna. In order to improve the pulse cancellation it would be necessary to use pulse shaping circuits tailored for the individual oscillator or to use two similar oscillators, one terminated in a matched load in order to obtain the reference pulses, and the other acting as the sensor itself. These techniques, however, add to the cost, complexity, and power consumption of the system, and therefore detract from any advantages to be gained from pulsed operation of self-detecting field sensors.

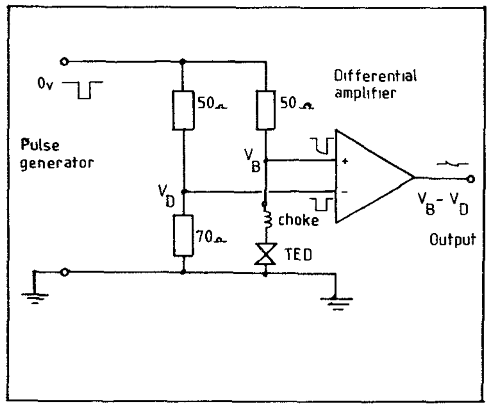

Fig. 12. The differential amplifier cancellation circuit used to detect the doppler signal, due to a moving target, in the bias circuit of the pulsed oscillator.

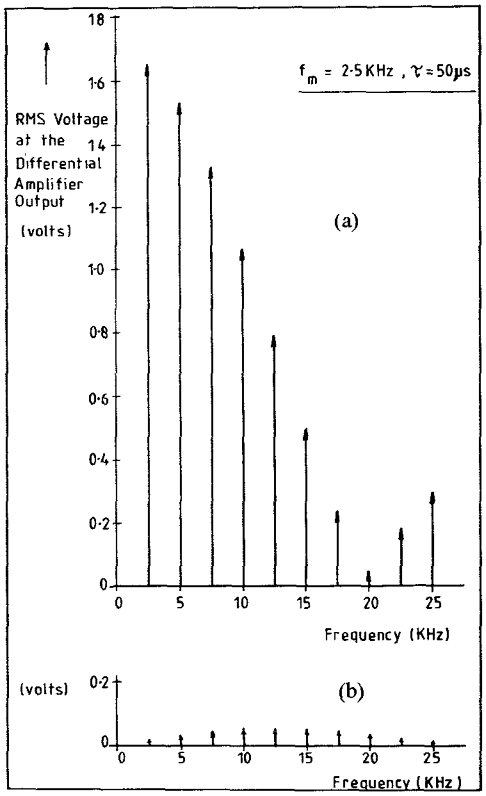

Fig. 13. Measured spectra of the pulse bias voltage waveform at the differential amplifier output (a) without the dummy load and (b) with pulse subtraction.

V. Conclusions

It has been shown that FM–CW radar techniques can be applied to low-cost self-detecting field sensors in order to improve their performance as doppler motion detectors. Experimental results have been described using bias-voltage tuned and varactor tuned transferred-electron oscillators which behave as load variation detectors when the output power is radiated and the bias current is sampled in a series resistor. In principle, linear FM–CW modulation patterns can be used in conjunction with self-detecting sensors in order to measure target range in addition to velocity, although the presence of large amplitude cross-modulation currents in the bias circuits at the modulation frequency and its harmonics makes it difficult to extract and measure the instantaneous beat frequencies. The problems of wave-shaping to produce linear FM patterns and the difficulties of handling multiple targets also make the technique impractical for use in low-cost sensors. However, a novel technique of environmental profiling has been proposed in order to exploit the response of a modulated field sensor to multiple stationary targets for use in a short-range surveillance system. The technique uses linearly modulated FM–CW sensors with digital FFT processing in order to form a spectrum or profile to represent a cluttered environment which can be compared with a previously stored data profile in order to detect any change occurring in the area under surveillance. The proposed system could measure the range of any disturbance and the use of digital processing could lead to a system which would be extremely versatile. The performance of the microwave sensors is not critical and these could be low-cost items so that surveillance over a wide area is feasible using any number of sensors and a single processor.

Experimental results have shown that sinusoidal FM–CW operation is a viable technique for eliminating false alarms due to unwanted targets in low-cost self-detecting sensors. The technique exploits the properties of the Bessel function dependence in the spectrum of the beat signal of a sinusoidally modulated sensor in order to discriminate against target range, and several possible schemes have been described for reducing the false alarm rate in short-range sensors. The range discrimination properties have been demonstrated using bias-voltage modulated and varactor modulated TEO's. Although wider tuning ranges were achieved in the varactor tuned circuit, both tuning methods were found to be suitable and the bias tuned oscillator yielded better tuning linearity. The bias tuned oscillator is also simpler and probably cheaper than a varactor tuned circuit, but its tuning characteristics are likely to be less predictable from one device to the next. A further advantage of the sinusoidal FM technique in a self-detecting sensor is the possibility of achieving better sensitivity for certain target ranges because of the $1/f$ noise power density spectrum characteristic of these devices.

The mechanism of pulsed operation in self-detecting sensors and the extraction of doppler information using a differential amplifier pulse cancellation circuit have been described. Target motion results in a pulse-amplitude-modulation waveform in the bias circuit of the oscillator and unmodulated pulses must be subtracted in a comparator circuit in order to isolate the baseband doppler component by means of a low-pass filter. The pulsed field sensor has a range cutoff property whereby targets at ranges greater than $\tau c/2$ (where τ is the pulse length) are not detected at all and this feature provides a means of eliminating false alarms due to distant targets. The effects of chirp in pulsed field sensors have been discussed, and the change in frequency during a pulse does not significantly affect the performance except in the case of the range-measuring FM-pulse system. However, experimental results obtained using a pulsed TEO show that temperature variations in the active device result in a variation in bias current during the pulse, which is detrimental to the use of pulse cancellation circuits where the reference pulses are derived from the applied voltage waveform by means of a dummy resistive load. In order to achieve sufficient pulse cancellation it is necessary to use a dummy oscillator or some sort of pulse shaping circuits which would add to the cost and power consumption of the system, and therefore detract from any advantages to be gained from pulsed operation of self-detecting sensors.

Acknowledgment

The authors would like to acknowledge the support of the Science Research Council and would also like to thank colleagues and staff at Leeds University and at RSRE Malvern for many useful discussions during the course of this work.

References

[1] R. D. Codd, "Recent trends in automotive radar," *Radio Electron. Eng.*, vol. 47, no. 10, pp. 472–476, Oct. 1977.
[2] Y-K. Wu and C. P. Tresselt, "Millimeter radar for highway collision avoidance," *Microwave J.*, vol. 20, no. 11, Nov. 1977.
[3] A. C. Prior and K. J. Warren, "A man portable radar for use by patrols," in *Proc. IEE 1973 Int. Conf. Radar, Present and Future*, Oct. 1973, pp. 384–394.
[4] R. H. Merriam and J. W. Rush, "Microwave doppler sensors," *Microwave J.*, vol. 17, no. 7, pp. 27–30, July 1974.
[5] S. Nagano and Y. Akaiwa, "Behavior of Gunn diode oscillator with a moving reflector as a self-excited mixer and a load variation detector," *IEEE Trans. Microwave Theory Tech.*, vol. MTT-19, pp. 906–910, Dec. 1971.
[6] M. Kotani and S. Mitsui, "Self-mixing effect of Gunn oscillator," *Electron. Commun. (Japan)*, vol. 55-B, no. 12, pp. 60–67, 1972.
[7] Y. Takayama, "Doppler signal detection with negative resistance diode oscillators," *IEEE Trans. Microwave Theory Tech.*, vol. MTT-21, pp. 89–94, Feb. 1973.
[8] M-S. Gupta, R. J. Lomax, and G. I. Haddad, "Noise contributions in self-mixing IMPATT-diode oscillators for short-range doppler radar applications," *IEEE Trans. Microwave Theory Tech.*, vol. MTT-22, pp. 37–43, Jan. 1974.
[9] J. R. East, H. Nguyen-Ba, and G. I. Haddad, "Design, fabrication, and evaluation of BARITT devices for doppler system applications," *IEEE Trans. Microwave Theory Tech.*, vol. MTT-24, pp. 943–948, Dec. 1976.
[10] P. A. Jefford, Modulation schemes in microwave field sensors," Ph.D. thesis, Univ. of Leeds, 1980.
[11] J. E. Saw, "Microwave doppler intruder alarms," *Mullard Tech. Commun.*, no. 131, pp. 44–52, July 1976.
[12] M. W. Hosking, "Microwave intruder alarm construction of doppler radar to detect movement," *Wireless World*, vol. 22, no. 7, pp. 36–39, July 1977.
[13] J. N. Holyoak, V. T. Rhyne, and P. S. Noe, "Improving volumetric intrusion security system reliability through the use of a digital processing technique," in *Proc. 1974 Carnahan Int. Crime Countermeasures Conf.*, pp. 64–67.
[14] B. W. Armstrong, R. Brown, E. J. Duffin, and J. A. C. Stewart, "Short-range microstrip doppler radar sensor using a BARITT diode," in *Technology Growth for the 80's, 1980 IEEE MTT-S Int. Microwave Symp. Dig.*, pp. 501–503.
[15] M. I. Skolnik, *Introduction to Radar Systems.* New York: McGraw-Hill, 1962, ch. 3.

[16] D. D. Tang and R. J. Lomax, "Bias-tuning and modulation characteristics of transferred-electron oscillators," *IEEE Trans. Microwave Theory Tech.*, vol. MTT-23, pp. 748–753, Oct. 1975.
[17] W. C. Tsai and F. J. Rosenbaum, "Amplitude and frequency modulation of a waveguide cavity CW Gunn oscillator," *IEEE Trans. Microwave Theory Tech.*, vol. MTT-18, pp. 877–884, Nov. 1970.
[18] G. King and M. P. Wasse, "Frequency modulation of Gunn effect oscillators," *IEEE Trans. Electron Devices*, vol. ED-14 (Corr.), pp. 717–718, Oct. 1967.

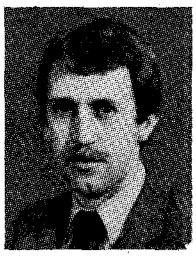

Peter A. Jefford was born in Manchester, England on August 18, 1955. He received the B.Sc. degree in electrical and electronic engineering from the University of Leeds in 1976 and completed a Ph.D. degree on modulation schemes in microwave field sensors at the same University in 1980.

Since 1980 he has been working at the Royal Signals and Radar Establishment, Malvern, England, engaged in microwave and millimeter-wave subsystems research.

Dr. Jefford is an associate member of the Institute of Electrical Engineers, London.

Michael J. Howes was born in Lowestoft, England, in 1941, and acquired his early education while working at a Government Fisheries Research Station where he was involved in the development of sector scanning sonar systems. He received the B.Sc. and Ph.D. degrees from the University of Leeds, England, in 1965 and 1967 respectively.

He is presently a Senior Lecturer in the Department of Electrical and Electronic Engineering at the University of Leeds, and has acted as consultant to a number of companies in the U.K. and U.S.A.

During the period 1981–1982 he was the Technical Director of MM Microwave, Ltd. His research interests are in the areas of microwave solid-state devices and systems in general, and his personal research work is currently associated with the design of MESFET amplifiers, oscillators, and mixers.

Dr. Howes is a Fellow of the Institute of Electrical Engineers and a member of the Institute of Physics.

Measurement and Modeling of the Apparent Characteristic Impedance of Microstrip

WILLIAM J. GETSINGER, FELLOW, IEEE

Abstract **—Voltage and current cannot be defined uniquely for microstrip except at zero frequency, and therefore microstrip has not been rigorously incorporated into circuit theory. However, in engineering practice, microstrip exhibits an apparent characteristic impedance, denoted here by *ZA*, that can be measured.**

Three methods of measuring *ZA* were devised and used in measuring three impedance levels of microstrip. These methods are described and experimental results presented. The measurements of *ZA* were found to be consistent with the power-current characteristic impedance definition of the approximate longitudinal-section electric (LSE) model of microstrip. Simple approximate formulas for representing *ZA* are also discussed.

I. Introduction

IMPEDANCE IS a fundamental concept in microwave circuit design because the impedances of circuit elements and their interconnections determine the distribution of power within a circuit. The ability of a microwave engineer to predict circuit performance will partially depend on the accuracy of the knowledge of impedances for available circuit elements.

This paper examines the frequency variation of the apparent characteristic impedance of a microstrip transmission line. From a practical viewpoint, the term "characteristic impedance" used here is the impedance parameter of a circuit-theory based model of a transmission line which is used in a circuit description with other elements to predict the actual performance of a physical circuit. An example is the parameter $Z0$ used in a computer-aided design (CAD) program, such as SUPER-COMPACT™. Microstrip is not a TEM line, and so voltage and current, and thus characteristic impedance, cannot be defined uniquely. The term "apparent characteristic impedance" is used to denote a parameter that describes how microstrip exchanges power with a TEM line, just as characteristic impedance is the parameter that determines how one TEM line exchanges power with another. The purpose of this

Manuscript received September 7, 1982; revised March 15, 1983. This paper is based on work performed at COMSAT Laboratories under the shared sponsorship of the Communications Satellite Corporation and the COMPACT Engineering Division of COMSAT General Integrated Systems Corporation.
The author is with COMSAT Laboratories, Clarksburg, MD 20871.

0018-9480/83/0800-0624$01.00 ©1983 IEEE